# Isotopic effects in the collision of CH+ with He

Ghofran Werfelli, Christian Balança, Thierry Stoecklin, Boutheïna Kerkeni, Nicole Feautrier

Monthly Notices of the ROYAL ASTRONOMICAL SOCIETY

MNRAS **468,** 2582–2589 (2017) doi:10.1093/mnras/stx675
Advance Access publication 2017 March 17

# Isotopic effects in the collision of $CH^+$ with He

Ghofran Werfelli,[1,2,3] Christian Balança,[1★] Thierry Stoecklin,[2] Boutheïna Kerkeni[1,3,4] and Nicole Feautrier[1]

[1]*LERMA, Observatoire de Paris, PSL Research University, CNRS-UMR8112, Sorbonne Universités, UPMC Univ. Paris 06, F-92195 Meudon, France*
[2]*Institut des Sciences Moléculaires, Université de Bordeaux, CNRS UMR 5255, F-33405 Talence Cedex, France*
[3]*Laboratoire de Physique de la Matière Condensée, Faculté des Sciences de Tunis, Campus Universitaire, 2092, Tunisia*
[4]*Institut Supérieur des Arts Multimédia de la Manouba, Université de la Manouba, 2010 la Manouba, Tunisia*

Accepted 2017 March 15. Received 2017 March 10; in original form 2017 January 11

## ABSTRACT

Deuterated species are proved to be helpful in understanding the physical and chemical properties in various astrophysical environments. The present study is dedicated to the rotational excitation of $CD^+$ by collision with $^4$He and to the comparison between $CD^+$–He and $CH^+$–He rate coefficients. Close coupling $CD^+$–He rotational cross-sections are calculated within the rigid-body approach for collision energies up to 3000 $cm^{-1}$ and the corresponding rate coefficients are evaluated for the transitions of levels up to $j = 10$ and temperatures up to 300 K. Significant differences are found between the rate coefficients of the two isotopologues.

**Key words:** molecular data – molecular processes – ISM: abundances.

## 1 INTRODUCTION

The methylidyne cation ($CH^+$) is a key species for chemistry studies in the interstellar medium (ISM). This ion was detected for the first time by Douglas & Herzberg (1941) in diffuse interstellar clouds and was then the target of a large number of subsequent observations. Nevertheless, its observed overabundance is not currently explained. Several mechanisms have been proposed to explain its formation, in particular the following reaction:

$$C^+ + H_2 \rightarrow CH^+ + H. \quad (1)$$

This reaction was the subject of numerous theoretical (Stoecklin & Halvick 2005; Halvick et al. 2007; Werfelli et al. 2015) and experimental (Plasil et al. 2011) studies. The recent theoretical results (Werfelli et al. 2015) calculated using a new high-quality potential energy surface (PES) are found in good agreement with the experimental data in the range 50–800 K. At lower temperature, however, the steep fall-off observed experimentally by Plasil et al. (2011) is not reproduced by the calculations.

The study of deuterated molecules in the interstellar medium has proved to be helpful in understanding the physical and chemical properties of cold and hot environments. In fact, the detected interstellar abundance of D atoms in molecules is much enhanced over the cosmic D/H abundance ratio, $1.5 \times 10^{-5}$ (Roberts & Millar 2000; Pety et al. 2005). This is due to small zero-point energy differences which ensure that deuterium is preferentially bonded in molecules compared to hydrogen. Fractionation can then be used to probe the history of interstellar matter if we know in detail the chemical kinetic processes by which it is incorporated into molecules. Observation of deuterated molecules is therefore a powerful way to get information on the formation and evolution of molecular clouds (Treviño-Morales et al. 2014). Gas phase deuterium chemistry was for example recently shown to be a useful tool to measure the age of clouds and prestellar cores (Pagani et al. 2015). In molecular clouds, deuterium is mainly found as molecular HD. In low-temperature dark clouds, the efficient transfer of deuterium from this reservoir can only occur by means of ion–molecule reactions and only by those involving HD which are fast enough to compete against electron recombination. These are the reactions with $H_3^+$ and its isotopologues which are all exothermic. In warmer environments, as for example the photodissociation region of the Orion Bar, these are the reactions of $CH_2^+$ and its isotopologues (Parise et al. 2009).

When looking at a possible production mechanism of $CD^+$ in molecular clouds, one could suggest a reaction (equation 1) starting from HD instead of $H_2$. However, this reaction is endothermic. In regions, where $CH^+$ is observed the production of $CD^+$ from the HD reservoir can be expected to be more efficient than the reaction

$$CH^+ + HD \rightarrow CD^+ + H_2 \quad (2)$$

as it is exothermic by approximately 90 K. Another possible mechanism would directly involve deuterium by the reaction

$$CH^+ + D \rightarrow CD^+ + H. \quad (3)$$

Reaction (2) may furthermore allow determining the equilibrium fractionation of $CD^+$ versus $CH^+$. If one makes the usual assumption that the rate coefficients for both directions are equal, except for a Boltzmann factor, $\exp(-\Delta E/k_B T)$, in the reverse direction, the fractionation has an exponential dependence on $1/T$. However, at very low temperatures, when the reactions become essentially irreversible, other destruction reactions of $CD^+$ become important.

★ E-mail: Christian.Balanca@obspm.fr

This simple gas-phase model can be described by the following equation:

$$\frac{[CD^+]}{[CH^+]} = \frac{k_f}{k_f \exp(-\Delta E/k_B T) + k_e[e^-] + \Sigma_i k_i [M_i]} \frac{[HD]}{[H_2]}, \quad (4)$$

where $k_f$ is the rate coefficient for formation via reaction (2), $k_e$ is the rate coefficient for dissociative recombination of $CD^+$ with electrons and $[e^-]$ is the fractional abundance of electrons, while $k_i$ $[M_i]$ represents the destruction of $CD^+$ by other species like CO, $H_2O$ and O, $[M_i]$ being the fractional abundance of species $i$ and $k_i$ the rate coefficient for its reaction with $CD^+$. The models of fractionation assume that both deuterium and hydrogen-bearing species react with the same species at the same rate (Roberts & Millar 2000). This is a very good approximation for ion–neutral reactions, whose rate coefficients depend only on the dipole moment and polarizability of the neutral. In this case, the rate coefficients should not vary by more than a few per cent when a D atom is substituted for an H. Conversely, for the reaction that proceeds via quantum tunnelling of the hydrogen atoms, their substitution by heavier deuterium atoms as in reaction (3) may reduce considerably the tunnelling rate coefficients (Bell et al. 1988).

From expression (4), we see that even if we take for $CD^+$ the data known for $CH^+$, much data about the destruction reaction rates of $CH^+$ are unknown and thus do not allow at this stage to propose an estimate of the fractionation of $CD^+$ versus $CH^+$. We conclude this discussion by noting that this simple gas-phase model furthermore does not include depletion on to grains which would reduce the gas-phase abundance of $CD^+$. Neither does it intend to be exhaustive about all the possibilities of formation and destruction of $CD^+$ but we hope that it will be of help in the future when $CD^+$ will be detected.

However, at the typical low ISM densities, the energy levels are not at local thermodynamical equilibrium. The modelling of molecular emission requires to know the collisional rate coefficients of the considered molecules with the most abundant species. Many theoretical and experimental results have been achieved in recent years for collisions with He, $H_2$ and with electrons (see Roueff & Lique 2013 and references therein) but few have concerned the deuterated species. It is generally assumed that the rate coefficients of the main isotopologue are a good approximation for the secondary isotopologues. This approximation, which could be acceptable for some systems involving heavy atoms, was found questionable in the case of $^{13}C/^{15}C$ substitution for CN–$H_2$ collisions (Flower & Lique 2012) and becomes non-realistic in the case of D/H substitution, as found for collisions of $H_2O/D_2O$ with $H_2$ (Scribano, Faure & Wiesenfeld 2010), NH/ND (Dumouchel et al. 2012) and HCN/DCN (Denis-Alpizar, Stoecklin & Halvick 2015) and to a lesser extent for $HCO^+/DCO^+$ (Buffa, Dore & Meuwly 2009; Buffa 2012) in collision with He. The rate coefficients involving two isotopic species were found to differ sometimes by more than a factor of 2–3, the rate coefficients being larger or smaller according to the species and to the considered transition and temperature. It is also important to notice that $H_2$ is the dominant collision partner in various astrophysical environments. It is often proposed to use He-rate coefficients with the appropriate reduced mass correction as an estimate of rate coefficients with *para*-$H_2(j = 0)$. This approximation may be used with caution as many results show that rate coefficients with He and $H_2$ differ by a factor of 2–3 according to the transitions. The inelastic rate coefficients of $CH^+$ with H have also been calculated. This system is however reactive and it was found (Werfelli et al. 2015) that rigid rotor calculations do not work for this system. Scaling of these data thus seems even more hazardous.

Recently, rotational inelastic excitation of $CH^+$ by collision with He has been theoretically studied (Stoecklin & Voronin 2008; Hammami et al. 2008; Turpin, Halvick & Stoecklin 2010). The first study (Hammami et al. 2008) was limited to the rigid-body approach and their surface did not include explicitly the long-range interaction which is important for ionic systems. From a 3D-PES including the long-range interactions and the close-coupling collisional approach, Turpin et al. (2010) have calculated cross-sections and rate coefficients for the transitions of levels up to $j = 5$ and temperatures up to 500 K. A comparison at 20 and 200 K of the $CH^+$–He rate coefficients, calculated using the same PES but with or without the rigid-body approximation, shows differences by 10–20 per cent on average between the two sets of data (Turpin et al. 2010). These differences were attributed to the unusual geometry of the He–$CH^+$ complex which is leading to unusual strong vibrational coupling (Stoecklin & Voronin 2008). Discrepancies by up to 33 per cent at 20 K, decreasing at 200 K, are found between the rigid-body results obtained by Hammami et al. (2008) and Turpin et al. (2010). They are mainly explained by the inclusion of the long-range charge-induced dipole interaction in the PES (Stoecklin & Voronin 2008) used by Turpin et al. (2010).

Strong isotopic effects were found at very low energies (less than a few $cm^{-1}$) for the collisions of $CH^+$ with $^4$He and $^3$He, while these differences disappear at higher energies. Conversely, there are no studies available for the isotopic effects upon substitution of H by D in the collision of $CH^+$ with $^4$He. Also, the present study provides the first rate coefficients for rotational excitation of $CD^+$ by $^4$He and a comparison between $CD^+$–He and $CH^+$–He rate coefficients.

The manuscript is organized as follows. In Section 2, we describe the methods and the parameters used to perform the scattering calculations, while the results are presented and compared with those of $CH^+$ in Section 3. Concluding remarks are given in Section 4.

## 2 METHODOLOGY

### 2.1 Potential energy surface

Within the Born–Oppenheimer approximation, the $CD^+$–He and $CH^+$–He electronic wavefunction are identical and only depend on the mutual distances of the atoms. The $CD^+$–He PES was derived from the one computed by Stoecklin & Voronin (2008). The $CH^+$–He *ab initio* energies were computed in the supermolecular approach at the BCCD(T) 'coupled cluster' level with the Brueckner orbitals (Handy et al. 1989). The a-cc-pVQZ basis set of Woon & Dunning (1993) was used, supplemented with the Tao & Pan (1992) bond functions placed at the mid-point between the He atom and the $CH^+$ centre of mass. At each geometry, the calculated energy was corrected for the basis set superposition error (BSSE) using the Boys & Bernardi (1970) counterpoise procedure. The analytical representation of the PES was obtained by using the reproducing kernel Hilbert space method (RKHS) (Ho & Rabitz 1996) which accurately describes the long-range part of the interaction. The global minimum of the PES is found to be $E = -513.573$ $cm^{-1}$ for Jacobi geometries $r = 2.13128$ $a_0$, $R = 4.1$ $a_0$ and $\theta = 86.0°$.

Assuming that the bond lengths vary only slightly between two isotopic species, we used in the present work a 'rigid rotor' approach for a C–D distance equal to the C–H equilibrium distance (2.13728 $a_0$). Then, the only difference between the $CD^+$–He and the $CH^+$–He PESs is the position of the centre of mass taken for the origin of the Jacobi coordinates used in the scattering calculations. For

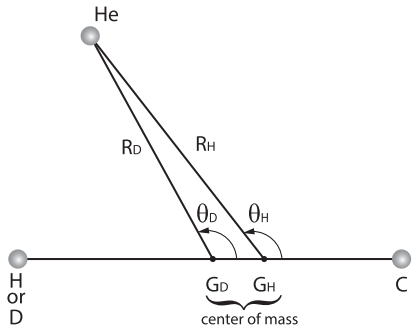


**Figure 1.** Jacobi coordinates for the $CH^+$–He and $CD^+$–He potential energy surfaces.

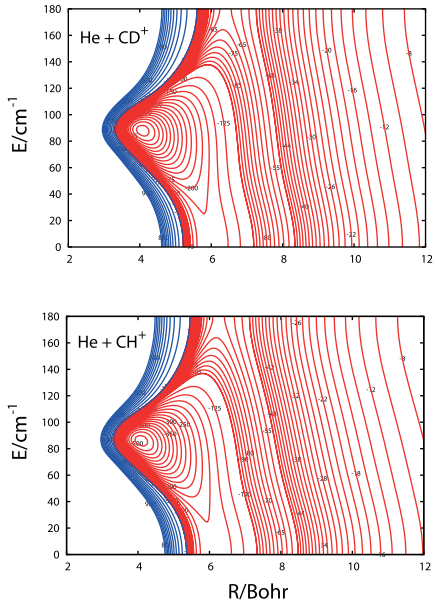


**Figure 2.** Contour plot of the He–$CH^+$ and of the He–$CD^+$ potential energy surfaces in Jacobi coordinates.

$CD^+$–He, we used new Jacobi coordinates $R_D$ and $\theta_D$ instead of $R_H$ and $\theta_H$ (Dumouchel et al. 2012) (see Fig. 1).

The two 2D-PES were finally fitted to the form of equation (5) which is suitable for use in achieving numerically efficient solutions to scattering calculations with the MOLSCAT code (Hutson & Green 1994). We used the procedure described by Werner et al. (1989), including expansion functions $P_l$ up to $l = 19$ to represent the large angular anisotropy:

$$V(R,\theta) = \sum_l V_l(R)\ P_l(\cos\theta). \qquad (5)$$

As a result of this fitting procedure, the $CH^+$–He PES differs by less than a fraction of $cm^{-1}$ from the analytic PES. The substitution of H by D has no visible effect on the general shape of the PES (see Fig. 2); however, the centre of mass displacement leads to different expansions (equation 5) of the $CD^+$–He and $CH^+$–He PESs. The dependence on $R$ of the first terms of the two expansions is displayed in Fig. 3. We note that the differences between the two expansions are very small for even $l$-values, but are particularly large for odd $l$-values, particularly for the $l = 1$ contribution. This reflects a larger odd anisotropy for the $CD^+$–He PES than for the $CH^+$–He PES that could influence the values of the corresponding rate coefficients.

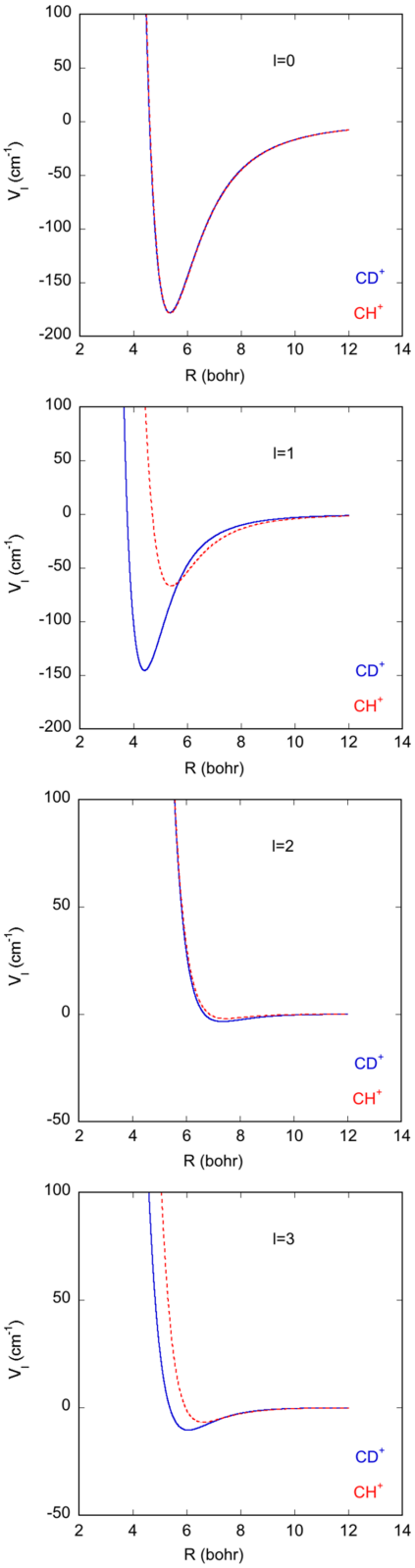


**Figure 3.** Plot of the first radial expansion coefficients $v_l(R)$ as a function of $R$. Solid lines denote $CD^+$–He while dashed lines denote $CH^+$–He. Distances $R$ in bohr and energies in $cm^{-1}$.

**Table 1.** $CD^+$ and $CH^+$ energy levels ($cm^{-1}$).

| $j$ | $CD^+$ | $CH^+$ |
|---|---|---|
| 0 | 0.0000 | 0.0000 |
| 1 | 15.1277 | 27.8559 |
| 2 | 45.3734 | 83.5347 |
| 3 | 90.7178 | 166.9702 |
| 4 | 151.1315 | 278.0636 |
| 5 | 226.5758 | 416.6825 |
| 6 | 317.0022 | 582.6620 |
| 7 | 422.3523 | 775.8038 |
| 8 | 542.5582 | 995.8767 |
| 9 | 677.5421 | 1242.6166 |
| 10 | 827.2167 | 1515.7262 |

### 2.2 Scattering calculations

Our aim is to calculate the He-collision rate coefficients for the first rotational levels of $CD^+$ ($v = 0$) and to compare the results with the CH$^+$–He data (Turpin et al. 2010, hereafter Paper I). For $CD^+$, the rotational constant (7.5646 $cm^{-1}$) is about two times smaller than the $CH^+$ (13.9307 $cm^{-1}$) (Sauer & Špirko 2013) and the energies of the $v = 1$ first excited vibrational level are 2739.6582 and 2035.3982 $cm^{-1}$ for $CH^+$ and $CD^+$, respectively. In this work, we assume that, at low temperatures, the coupling between the first $v = 0$ rotational states and the $v = 1$ vibrational state is negligible. This approximation should work better for collisions of $CD^+$ than for $CH^+$ due to the lower rotational constant of the former as can be seen in Table 1 that displays the energies of the first 10 rotational levels of $CH^+$ and $CD^+$. The energies of the rotational levels were computed with the use of the spectroscopic constants given by Sauer & Špirko (2013).

The $CD^+$ close-coupling calculations were carried out with the MOLSCAT code (Hutson & Green 1994) using the log-derivative propagator. The integration parameters were chosen to ensure convergence of the cross-sections between the first 10 rotational levels over this range. For all energies, the minimum and maximum integration distances and the propagation step size (parameter STEPS) were adjusted in order to ensure the convergence of the calculations. The value of this STEPS parameter decreases from 40 for energies less than 100 $cm^{-1}$ to 20 for larger energies. At energies lower than 200 $cm^{-1}$, the $CD^+$ rotational basis set was taken equal to 15 while the rotational basis was extended to $j = 20$ at larger energies. Convergence of the cross-section as a function of the total angular momentum was automatically checked by the MOLSCAT code, the maximum value used in the calculation is 160 for the largest energies.

The scattering calculations were carried out on a grid of the total energies $E_{\rm tot}$ as follows:

$$E_{\rm tot} = E_c + E_j, \tag{6}$$

where $E_c$ is the initial kinetic energy and $E_j$ is the rotational energy of level $j$. We used a total energy grid with a variable step. For energies below 500 $cm^{-1}$ the step was equal to 0.1 $cm^{-1}$, then between 500 and 800 $cm^{-1}$ it was increased to 0.5 $cm^{-1}$, and to 10 and 50 $cm^{-1}$ for energy intervals from 800 to 1000 $cm^{-1}$ and 1000 to 3000 $cm^{-1}$, respectively. Using this energy grid, the resonances (Feshbach and shape) that may appear in the cross-sections at low energies are well represented.

The thermal rate coefficients for excitation and de-excitation transitions at temperature $T$ are then calculated by averaging the cross-sections over a Boltzmann distribution of the kinetic energy:

$$k_{\alpha\to\beta}(T) = \left(\frac{8}{\pi\mu k_{\rm B}^3 T^3}\right)^{\frac{1}{2}} \int_0^\infty \sigma_{\alpha\to\beta}\, E_c\, e^{-\frac{E_c}{k_{\rm B}T}}\, dE_c, \tag{7}$$

where $\sigma_{\alpha\to\beta}$ is the cross-section from an initial rotational level $\alpha$ and a final level $\beta$, $\mu$ is the reduced mass of the system and $k_{\rm B}$ is the Boltzmann constant.

For comparison purposes with the CH$^+$–He rigid rotor (RR) results (see Paper I) obtained from the same PES but with a different scattering code, calculations were also carried out for CH$^+$–He-collisions using the MOLSCAT code and the CD$^+$–He integration parameters. The reduced mass of the CH$^+$–He system is $\mu = 3.06125$ whereas the reduced mass of the CD$^+$–He system is $\mu = 3.11338$. The agreement between our CH$^+$–He rate coefficients at 20 and 200 K and the RR-values obtained by Turpin et al. (2010) is good, with relative differences less than 2 per cent apart for the small $j = 5 \rightarrow 0$ rate coefficient for which the difference reaches 5 per cent. These differences may be due to the use of different scattering parameters and in particular to the different $CH^+$ employed basis sets.

## 3 RESULTS AND DISCUSSION

### 3.1 CD$^+$–He cross-sections and rate coefficients

The results obtained for collisions of $CH^+$ by He have been presented in details in Paper I. In this section, we only focus on the rotational excitation of $CD^+$ by He. We have obtained the cross-sections for the first 10 levels of $CD^+$.

Fig. 4 shows the elastic and rotational de-excitation cross-sections out of the $j = 5$ $CD^+$ level as a function of the kinetic energy. As previously noticed for CH$^+$–He collisions, a resonance regime characterized by numerous overlapping resonances red superimposed on a regular decay is found at collisional energies up to approximatively 500 $cm^{-1}$. This is related to the presence of an attractive potential well which allows for the He atom to be temporarily trapped before dissociation of the collisional complex. The same feature is found for all other transitions.

By performing an average of the cross-sections over a Boltzmann distribution of the kinetic energy, we obtain the rate coefficients for temperatures up to 300 K. The thermal dependence of the

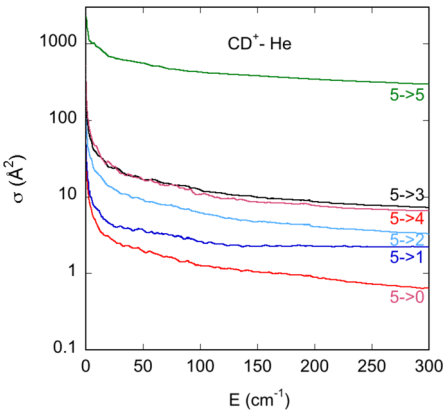


**Figure 4.** Rotational elastic and de-excitation cross-sections (in Å$^2$) of $CD^+$ ($v = 0, j = 5$) in collision with He as a function of the kinetic energy in $cm^{-1}$.

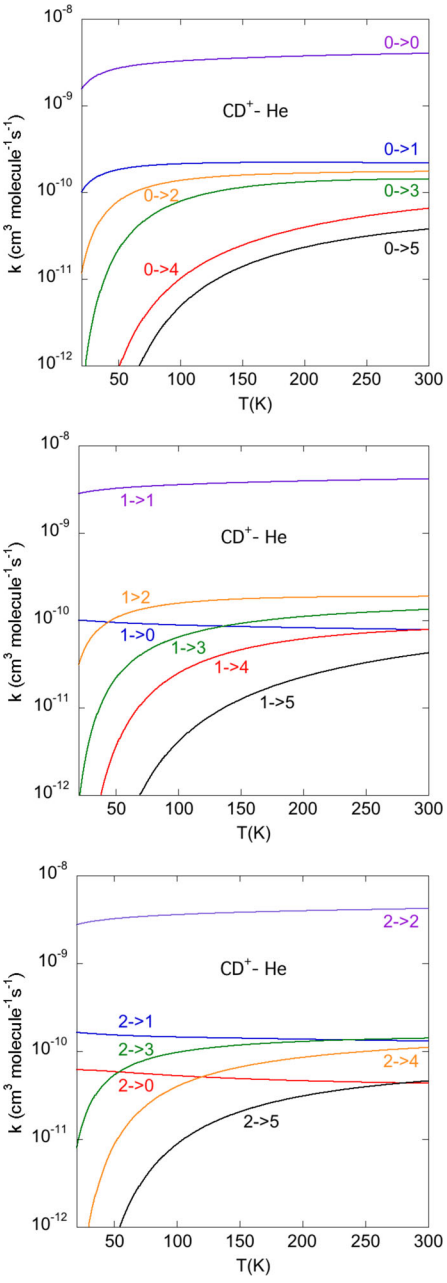


**Figure 5.** Rotational elastic, excitation and de-excitation rate coefficients out of the $j = 0 - 2$ levels of $CD^+$ in collision with He as a function of temperature.

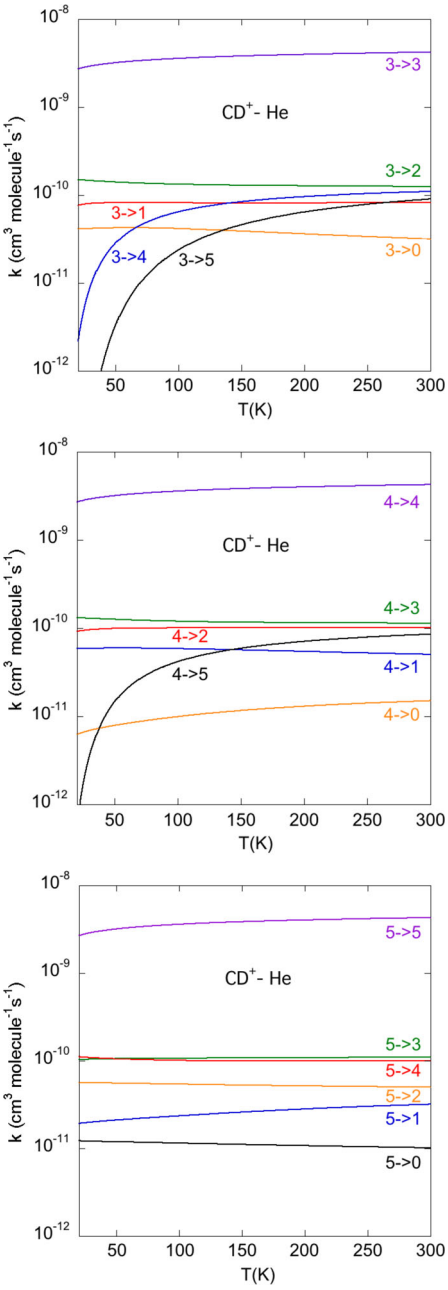


**Figure 6.** Rotational elastic, excitation and de-excitation rate coefficients out of the $j = 3 - 5$ levels of $CD^+$ in collision with He as a function of temperature.

$CD^+$–He rate coefficients is illustrated in Figs 5 and 6. One observes first that the de-excitation rate coefficients are almost constant over the considered temperature range. This could be anticipated on the basis of Langevin theory for ion–neutral interactions. The excitation rates increase monotonically as a function of temperature. From Figs 5 and 6, one can also see that the general trend of the rate coefficients is to decrease as $\Delta j$ increases, as expected. This effect is well illustrated in Fig. 7 which displays the de-excitation rate coefficients $k_{j\rightarrow j'}$ ($j' = 0$, 1) at temperature $T = 200$ K, out of level $j$ up to $j = 10$.

The values of our calculated rate coefficients for the rotational de-excitation of $CD^+$ ($j = 1$, 2, 3, 4, 5) are given in Table 2 for temperatures ranging from 1 to 300 K.

### 3.2 Comparison between $CH^+$–He and $CD^+$–He rate coefficients

It is often assumed that collisional rate coefficients of the main isotopologue can be used to estimate rate coefficients for secondary isotopologues. As previously pointed out, this approximation is questionable for H/D substitution. The comparison between $CH^+$–He and $CD^+$–He is performed between de-excitation rate coefficients to avoid threshold effects existing when excitation rate coefficients are considered.

We report in Figs 8 and 9 $CH^+$ and $CD^+$ de-excitation rate coefficients, out of levels $j = 2$ and $j = 3$, respectively, calculated within the same rigid rotor approximation. Also shown in these figures are the close-coupling $CH^+$–He rate coefficients (see Paper I). As

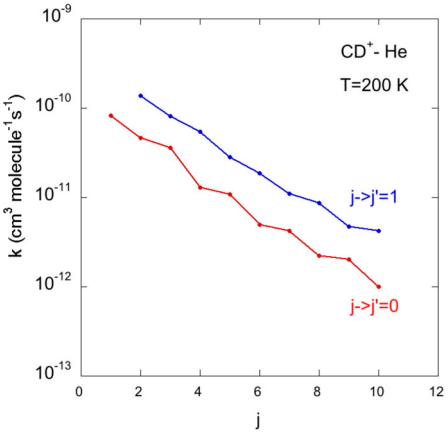


**Figure 7.** Inelastic CD$^+$–He de-excitation rate coefficients at 200 K for transitions out of the $j$ levels towards $j' = 0$ and $j' = 1$.

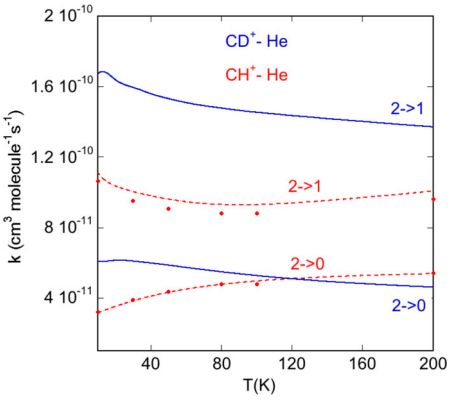


**Figure 8.** Rate coefficients from $j = 2$ state of CD$^+$ (solid lines) or CH$^+$ (dashed lines) induced by collisions with He. The red dots correspond to the close-coupling values reported by Turpin et al. (2010).

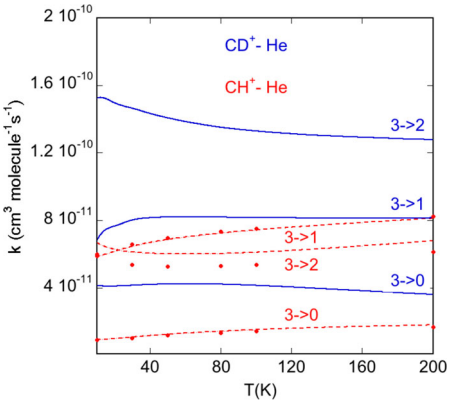


**Figure 9.** Rate coefficients from $j = 3$ state of CD$^+$ (solid lines) or CH$^+$ (dashed lines) induced by collisions with He. The red dots correspond to the close-coupling values reported by Turpin et al. (2010).

previously noticed, the CH$^+$–He rigid body (RR) and close-coupling rate coefficients differ, with differences ranging from a few per cent up to 20–30 per cent according to the transition. However, it can be considered that the rigid body approach provides a correct order of magnitude of the rate coefficients.

At low temperatures, one can see in Figs 8 and 9 that the CH$^+$ and CD$^+$ rate coefficients differ by large factors, the rates for the deuterated species being systematically higher than those for the hydrogenated isotopologue. This effect decreases progressively at higher temperatures and even gets reversed for some transitions ($j = 2 \rightarrow 0$ for example). In Table 3, we report CH$^+$ and CD$^+$ de-excitation rate coefficients at 20 and 200 K and the ratio CD$^+$–He/CH$^+$–He. At 20 K, the ratio varies from 0.69 up to 12.4, and it remains relatively smaller at 200 K. This behaviour can be caused by several factors: the difference of the reduced mass, the large difference between the energy levels and the change of the centre of mass of the PES. Due to the small change of the reduced mass, it clearly appears that the main factors are the displacement of the centre of mass in CD$^+$–He collisions and the smaller energy distance of the CD$^+$ levels; this last factor could be the major cause of the CD$^+$ larger rate coefficients at low temperatures. In the studies of rotational de-excitation by He of NH and ND (Dumouchel et al. 2012) and HCN/DCN (Denis-Alpizar et al. 2015), the ratios of the rate coefficients of the deuterated and hydrogenated systems exhibit such large variations depending on the transition. As a conclusion, one has to consider the different PES as well as the different rotational structure caused by H/D substitution in order to determine accurate

**Table 2.** Rate coefficients[a,b] at temperature $T$ (K) for rotational de-excitation of CD$^+$ in collision with He.

| $i \rightarrow j$ | 1.0 | 10 | 30 | 50 | 80 | 100 | 200 | 300 |
|---|---|---|---|---|---|---|---|---|
| 1→0 | 9.599(−11) | 1.004(−10) | 9.899(−11) | 9.455(−11) | 9.044(−11) | 8.851(−11) | 8.216(−11) | 7.819(−11) |
| 2→0 | 6.495(−11) | 6.095(−11) | 6.090(−11) | 5.862(−11) | 5.485(−11) | 5.269(−11) | 4.617(−11) | 4.317(−11) |
| 2→1 | 1.437(−10) | 1.670(−10) | 1.595(−10) | 1.531(−10) | 1.477(−10) | 1.453(−10) | 1.370(−10) | 1.303(−10) |
| 3→0 | 4.330(−11) | 4.150(−11) | 4.160(−11) | 4.243(−11) | 4.229(−11) | 4.155(−11) | 3.618(−11) | 3.156(−11) |
| 3→1 | 3.848(−11) | 6.793(−11) | 8.026(−11) | 8.209(−11) | 8.200(−11) | 8.178(−11) | 8.161(−11) | 8.207(−11) |
| 3→2 | 1.420(−10) | 1.524(−10) | 1.464(−10) | 1.407(−10) | 1.351(−10) | 1.330(−10) | 1.278(−10) | 1.252(−10) |
| 4→0 | 5.235(−12) | 5.491(−12) | 6.897(−12) | 7.877(−12) | 9.134(−12) | 9.911(−12) | 1.300(−11) | 1.500(−11) |
| 4→1 | 5.500(−11) | 5.886(−11) | 5.900(−11) | 5.953(−11) | 5.920(−11) | 5.860(−11) | 5.441(−11) | 5.036(−11) |
| 4→2 | 8.016(−11) | 8.674(−11) | 9.579(−11) | 9.928(−11) | 1.006(−10) | 1.008(−10) | 1.012(−10) | 1.019(−10) |
| 4→3 | 1.279(−10) | 1.337(−10) | 1.294(−10) | 1.260(−10) | 1.217(−10) | 1.197(−10) | 1.153(−10) | 1.142(−10) |
| 5→0 | 1.730(−11) | 1.286(−11) | 1.206(−11) | 1.190(−11) | 1.166(−11) | 1.150(−11) | 1.074(−11) | 1.015(−11) |
| 5→1 | 2.227(−11) | 1.906(−11) | 1.993(−11) | 2.107(−11) | 2.254(−11) | 2.350(−11) | 2.814(−11) | 3.189(−11) |
| 5→2 | 5.720(−11) | 5.700(−11) | 5.602(−11) | 5.555(−11) | 5.465(−11) | 5.406(−11) | 5.170(−11) | 4.982(−11) |
| 5→3 | 1.053(−10) | 1.024(−10) | 1.040(−10) | 1.055(−10) | 1.065(−10) | 1.069(−10) | 1.084(−10) | 1.101(−10) |
| 5→4 | 1.415(−10) | 1.175(−10) | 1.083(−10) | 1.051(−10) | 1.021(−10) | 1.010(−10) | 9.951(−11) | 1.003(−10) |

[a]In units of cm$^3$ molecule$^{-1}$ s$^{-1}$;
[b]a(−b) means a × $10^{-b}$.

**Table 3.** Comparison between the rate coefficients[a] (cm$^3$ molecule$^{-1}$ s$^{-1}$) of $CD^+$ and $CH^+$ in collision with He. The ratio corresponds to $k_{CD^+-He}/k_{CH^+-He}$.

| | $T = 20$ K | | | $T = 200$ K | | |
|---|---|---|---|---|---|---|
| $i \rightarrow j$ | $CD^+$–He | $CH^+$–He | Ratio | $CD^+$–He | $CH^+$–He | Ratio |
| 1→0 | 1.014(−10) | 7.472(−11) | 1.35 | 8.216(−11) | 9.509(−11) | 0.86 |
| 2→0 | 6.133(−11) | 3.511(−11) | 1.74 | 4.617(−11) | 5.378(−11) | 0.86 |
| 2→1 | 1.638(−10) | 1.035(−10) | 1.58 | 1.370(−10) | 1.005(−10) | 1.36 |
| 3→0 | 4.116(−11) | 1.002(−11) | 4.11 | 3.618(−11) | 1.810(−11) | 1.99 |
| 3→1 | 7.666(−11) | 6.173(−11) | 1.24 | 8.161(−11) | 8.134(−11) | 1.00 |
| 3→2 | 1.496(−10) | 6.297(−11) | 2.38 | 1.278(−10) | 6.801(−11) | 1.87 |
| 4→0 | 6.253(−12) | 9.028(−12) | 0.69 | 1.300(−11) | 8.403(−12) | 1.54 |
| 4→1 | 5.854(−11) | 1.636(−11) | 3.57 | 5.441(−11) | 1.767(−11) | 3.07 |
| 4→2 | 9.208(−11) | 8.952(−11) | 1.03 | 1.012(−10) | 9.270(−11) | 1.09 |
| 4→3 | 1.313(−10) | 3.003(−11) | 4.37 | 1.153(−10) | 3.956(−11) | 2.91 |
| 5→0 | 1.222(−11) | 9.811(−13) | 12.4 | 1.074(−11) | 1.421(−12) | 7.55 |
| 5→1 | 1.929(−11) | 2.234(−11) | 0.86 | 2.814(−11) | 2.078(−11) | 1.35 |
| 5→2 | 5.627(−11) | 6.895(−12) | 8.16 | 5.170(−11) | 9.490(−12) | 5.44 |
| 5→3 | 1.030(−10) | 8.626(−11) | 1.19 | 1.084(−10) | 8.572(−11) | 1.26 |
| 5→4 | 1.111(−10) | 1.789(−11) | 6.21 | 9.951(−11) | 2.316(−11) | 4.29 |

[a] a(−b) means a × $10^{-b}$

rate coefficients for the deuterated isotopologues, in agreement with previous works on this substitution.

The complete set of (de-)excitation rate coefficients will be made available through the LAMDA (Schöier et al. 2010) and BASECOL (Dubernet et al. 2013) data bases.

## 4 SUMMARY AND CONCLUSION

The rotational excitation of $CD^+$ by collision with He has been investigated for the first time within the rigid rotor approach. We have obtained $CH^+$ and $CD^+$ rate coefficients for transitions involving levels up to $j = 10$ and temperatures ranging from 5 to 300 K. From a comparison with previous work (Paper I), the present $CH^+$–He rate coefficients agree within a few per cent with the rigid rotor values whereas differences up to 20 per cent exist when the present data are compared with the close-coupling results. These differences are due to the coupling with the $v = 1$ vibrational $CH^+$ level. However, it should be noted that the coupling with $v = 1$ is practically negligible for the 10 lowest levels of $CD^+$ as a result of the smallest rotational constant. So, rigid-body results for $CD^+$ can be considered as reliable for levels up to $j = 10$ whereas already published $CH^+$ data (Paper I) should preferably be used. For both $CH^+$ and $CD^+$ systems, no strong propensity rule was obtained; however, as expected, the rate coefficients gradually decrease with increasing $\Delta j$.

The $CH^+$ and $CD^+$ rate coefficients were compared in details and large differences are found between the two sets of data. These differences may be explained by the large difference between the rotational structure of the two species as well as by the different angular expansion of their interaction with He atoms. From this comparison, it clearly appears that one has to be careful when using inelastic rate coefficients of the main isotopologue to interpret observations of the deuterated isotopologue as differences can reach factors between 1 and 8 according to the transition.

## ACKNOWLEDGEMENTS

This work was supported by the program Physique et Chimie du Milieu Interstellaire (PCMI) funded by CNRS and CNES. GW also gratefully acknowledges support from the European CM 1401 COST action and from El Manar University (Tunis). Part of the calculations were performed using HPC resources from GENCI-IDRIS and on work stations from Paris Observatory. This work was granted access to the HPC resources of [TGCC/CINES/IDRIS] under the allocation 2015047344 made by GENCI.

## REFERENCES

Bell M. B., Avery L. W., Matthews H. E., Feldman P. A., Watson J. K. G., Madden S. C., Irvine W. M., 1988, ApJ, 326, 924
Boys S. F., Bernardi F., 1970, Mol. Phys., 19, 553
Buffa G., 2012, MNRAS, 421, 719
Buffa G., Dore L., Meuwly M., 2009, MNRAS, 397, 1909
Denis-Alpizar O., Stoecklin T., Halvick P., 2015, MNRAS, 453, 1317
Douglas A. E., Herzberg G., 1941, ApJ, 94, 381
Dubernet M.-L. et al., 2013, A&A, 553, A50
Dumouchel F., Kłos J., Toboła R., Bacmann A., Maret S., Hily-Blant P., Faure A., Lique F., 2012, J. Chem. Phys., 137, 114306
Flower D. R., Lique F., 2012, MNRAS, 446, 1750
Halvick P., Stoecklin T., Larregaray P., Bonnet L., 2007, Phys. Chem. Chem. Phys., 9, 582
Hammami K., Owono Owono L. C., Jaidane N., Ben Lakhdar Z., 2008, J. Mol. Struct.:THEOCHEM, 853, 18
Handy N. C., Pople J. A., Head-Gordon M., Raghavachari K., Trucks G. W., 1989, Chem. Phys. Lett., 164, 185
Ho T.-S., Rabitz H., 1996, J. Chem. Phys., 104, 2584
Hutson J. M., Green S., 1994, molscat computer code, version 14 (1994), distributed by Collaborative Computational Project No. 6 of the Engineering and Physical Sciences Research Council (UK)
Pagani L., Lesaffre P., Roueff E., Jorfi M., Honvault P., Gonzalez-Lezana T., Faure A., 2015, Phil. Trans. R. Soc. A, 370, 5200
Parise B., Leurini S., Schilke P., Roueff E., Thorwirth S., Lis D. C., 2009, A&A, 508, 737
Pety J., Teyssier D., Fossé D., Gerin M., Roueff E., Abergel A., Habart E., Cernicharo J., 2005, A&A, 435, 885
Plasil R., Mehner T., Dohnal P., Kotrik T., Glosik J., Gerlich D., 2011, A&A, 737, 60
Roberts H., Millar T. J., 2000, A&A, 361, 388
Roueff E., Lique F., 2013, Chem. Rev., 113, 8906
Sauer S. P. A., Špirko V., 2013, J. Chem. Phys., 138, 024315
Schöier F., van der Tak F., van Dishoeck E., Black J., 2010, Astrophysics Source Code Library, record ascl:1010.077
Scribano Y., Faure A., Wiesenfeld L., 2010, J. Chem. Phys., 133, 231105

Stoecklin T., Halvick P., 2005, Phys. Chem. Chem. Phys., 7, 2446
Stoecklin T., Voronin A., 2008, Eur. Phys. J. D, 46, 259
Tao F. M., Pan Y. K., 1992, J. Chem. Phys., 97, 4989
Treviño-Morales S. P. et al., 2014, A&A, 569, A19
Turpin F., Halvick P., Stoecklin T., 2010, J. Chem. Phys, 132, 214305
Werfelli G., Halvick P., Honvault P., Kerkeni B., Stoecklin T., 2015, J. Chem. Phys., 143, 114304
Werner H.-J., Follmeg B., Alexander M. H., Lemoine D., 1989, J. Chem. Phys., 91, 5425
Woon D. E., Dunning T. H., Jr, 1993, J. Chem. Phys., 98, 1358

This paper has been typeset from a TEX/LATEX file prepared by the author.